
Title: 3GPP 25.996 v6.0.0 "Spatial Channel Model for Multiple-Input Multiple-Output Simulations"

Source: WI Editor (Lucent Technologies)

Agenda Item: 9.1.3

Document for: Information

The TR version attached was presented in RAN1#31 (R1-030347) as the output of SCM ad hoc. RAN1 decided to forward it to RAN#19 to be presented for approval but following some email discussions on the reflector and within the SCM ad hoc it was agreed that this TR would be presented to RAN#19 for information.

Presentation of Specification to TSG or WG

Presentation to: TSG RAN Meeting #19

Document for presentation: TR 25.996, Version 6.0.0

Presented for: Information

Abstract of document:

This document is part of the RAN WI '**Multiple Input Multiple Output work item**' and contains the Spatial Channel Model which were address in the SCM ad hoc as part of the harmonisation meeting between 3GPP and 3GPP2.

Based on the last SCM ad hoc some minor changes are still needed before approving the document.

Outstanding Issues:

SCM ad hoc will finish its work by the end of March and agree a final version.

Contentious Issues:

3GPP TR 25.996 V 6.0.0(2003-05)

Technical Report

3rd Generation Partnership Project; Technical Specification Group Radio Access Network; Spatial Channel Model for Multiple-Input Multiple Output Simulations (Release 6)



The present document has been developed within the 3rd Generation Partnership Project (3GPP™) and may be further elaborated for the purposes of 3GPP.

The present document has not been subject to any approval process by the 3GPP Organizational Partners and shall not be implemented.

This Specification is provided for future development work within 3GPP only. The Organizational Partners accept no liability for any use of this Specification.

Specifications and reports for implementation of the 3GPP™ system should be obtained via the 3GPP Organizational Partners' Publications Offices.

3GPP

Postal address

3GPP support office address

650 Route des Lucioles - Sophia Antipolis
Valbonne - FRANCE

Tel.: +33 4 92 94 42 00 Fax: +33 4 93 65 47 16

Internet

<http://www.3gpp.org>

Copyright Notification

No part may be reproduced except as authorized by written permission.
The copyright and the foregoing restriction extend to reproduction in all media.

© 2001, 3GPP Organizational Partners (ARIB, CWTS, ETSI, T1, TTA, TTC).
All rights reserved.

1		
2	CONTENTS	
3	Foreword	
4	1.1 Scope	
5	1.2 References.....	
6	1.3 Definitions, symbols, and abbreviations.....	
7	2 Spatial Channel Model for Calibration Purposes.....	
8	2.1 Purpose	
9	2.2 Link Level Channel Model Parameter Summary.....	
10	2.3 Spatial Parameters per Path.....	
11	2.4 BS and MS Array Topologies.....	
12	2.5 Spatial Parameters for the BS	
13	2.5.1 BS Antenna Pattern.....	
14	2.5.2 Per Path BS Angle Spread (AS)	1
15	2.5.3 Per Path BS Angle of Arrival.....	1
16	2.5.4 Per Path BS Power Azimuth Spectrum.....	1
17	2.6 Spatial Parameters for the MS.....	1
18	2.6.1 MS Antenna Pattern	1
19	2.6.2 Per Path MS Angle Spread (AS)	1
20	2.6.3 Per Path MS Angle of Arrival	1
21	2.6.4 Per Path MS Power Azimuth Spectrum.....	1
22	2.6.5 MS Direction of Travel.....	1
23	2.6.6 Per Path Doppler Spectrum.....	1
24	2.7 Generation of Channel Model.....	1
25	2.8 Calibration and Reference Values.....	1
26	3 Spatial Channel Model for simulations.....	1
27	3.1 General definitions, parameters, and assumptions.....	1
28	3.2 Environments.....	1
29	3.3 Generating User Parameters	2
30	3.3.1 Generating user parameters for urban macrocell and suburban macrocell environments	2
31		
32	3.3.2 Generating user parameters for urban microcell environments.....	2

1 3.4 Generating channel coefficients 2

2 3.5 Optional system simulation features 2

3 3.5.1 Polarized arrays 2

4 3.5.2 Far scatterer clusters 2

5 3.5.3 Line of sight 2

6 3.5.4 Urban canyon 2

7 3.6 Correlation Between Channel Parameters 3

8 3.7 Modeling intercell interference 3

9 3.8 System Level Calibration 3

10 Annex A: MMSE receiver description 4

11 Annex B: Change history 4

12

1 FOREWORD

2 This Technical Report has been produced by the 3rd Generation Partnership Project (3GPP)
3 The contents of the present document are subject to continuing work within the TSG and
4 change following formal TSG approval. Should the TSG modify the contents of the pr
5 document, it will be re-released by the TSG with an identifying change of release date a
6 increase in version number as follows:

7 Version x.y.z

8 where:

9 x the first digit:

10 1 presented to TSG for information;

11 2 presented to TSG for approval;

12 3 or greater indicates TSG approved document under change control.

13 y the second digit is incremented for all changes of substance, i.e. technical enhancements, correction
14 updates, etc.

15 z the third digit is incremented when editorial only changes have been incorporated in the document

16

17 1.1 Scope

18 This document details the current discussion of the combined 3GPP-3GPP2 Spatial Ch
19 Ad-hoc group. A similar document, developed independently in the 3GPP2 Spatial Ch
20 Modeling Ad-hoc group, was used for reference.

21 The scope of the 3GPP-3GPP2 SCM AHG is to develop and specify parameters and me
22 associated with the spatial channel modeling that are common to the needs of the 3GP
23 3GPP2 organizations (harmonization). The scope includes development of specifications f

24 System level evaluation.

25 Within this category, a list of four focus areas are identified, however the emphasis of the
26 AHG work is on items a & b.

27 a. Physical parameters (e.g. power delay profiles, angle spreads, dependencies be
28 parameters)

29 b. System evaluation methodology.

30 c. Antenna arrangements, reference cases and definition of minimum requirements.

31 d. Some framework (air interface) dependent parameters.

32 Link level evaluation.

33 The link level models are defined only for calibration purposes. It is a common view with
34 group that the link level simulation assumptions will not be used for evaluation
35 comparison of proposals.

1 **1.2 References**

2 The following documents contain provisions which, through reference in this text, cons
3 provisions of the present document.

4 ?? References are either specific (identified by date of publication, edition number, vers
5 number, etc.) or non-specific.

6 ?? For a specific reference, subsequent revisions do not apply.

7 ?? For a non-specific reference, the latest version applies. In the case of a reference to
8 3GPP document (including a GSM document), a non-specific reference implicitly ref
9 the latest version of that document *in the same Release as the present document*.

10 [1] L. Greenstein, V. Erceg, Y. S. Yeh, M. V. Clark, "A New Path-Gain/Delay-Spread Propa
11 Model for Digital Cellular Channels," IEEE Transactions on Vehicular Technology, VO:
12 NO.2, May 1997, pp.477-485.

13 [2] E. Sousa, V. Jovanovic, C. Daigneault, "Delay Spread Measurements for the Digital C
14 Channel in Toronto," IEEE Transactions on Vehicular Technology, VOL. 43, NO.4, Nov
15 pp.837-847.

16 [3] L. M. Correia, Wireless Flexible Personalized Communications, COST 259: European C
17 operation in Mobile Radio Research, Chichester: John Wiley & Sons, 2001.

18 **1.3 Definitions, symbols, and abbreviations**

19 In this document the following are terms that are commonly used interchangeably ar
20 equivalent. To promote consistency, the term on the left will be preferred in this docu
21 unless otherwise stated.

22 MS = Mobile Station = UE = User Equipment = Terminal = Subscriber Unit

23 BS = Base Station = Node-B = BTS

24 AS = Angle Spread = Azimuth Spread = θ_{AS}

25 DS = delay spread = τ_{DS}

26 LN = lognormal shadow fading = σ_{LN}

27 Path = Ray

28 Path Component = Sub-ray

29 PAS = Power Azimuth Spectrum

30 DoT = Direction of Travel

31 AoA = Angle of Arrival

32 AoD = Angle of Departure

33 PDP = Power Delay Profile

1 2 SPATIAL CHANNEL MODEL FOR CALIBRATION PURPOSES

2 This section describes physical parameters for link level modeling for the purpose
3 calibration.

4 2.1 Purpose

5 Link level simulations alone will not be used for algorithm comparison because they reflect
6 one snapshot of the channel behavior. Furthermore, they do not account for system attributes
7 such as scheduling and HARQ. For these reasons, link level simulations do not allow
8 conclusions about the typical behavior of the system. Only system level simulations
9 achieve that. Therefore we require system level simulations for the final algorithm comparison.

10 Link level simulations will not be used to compare performance of different algorithms. Rather
11 they will be used only for calibration, which is the comparison of performance results from
12 different implementations of a given algorithm.

13 2.2 Link Level Channel Model Parameter Summary

14 The table below summarizes the physical parameters to be used for link level modeling.

1

Model		Case I	Case II	Case III	Case IV				
Corresponding 3GPP Designator*		Case B	Case C	Case D	Case A				
Corresponding 3GPP2 Designator*		Model A, D, E	Model C	Model B	Model F				
PDP		Modified Pedestrian A	Vehicular A	Pedestrian B	Single Path				
# of Paths		1) 4+1 (LOS on, K = 6dB) 2) 4 (LOS off)	6	6	1				
Relative Path Power (dB)	Delay (ns)	1) 0.0	0	0,0	0	0.0	0	0	0
		2) -Inf							
		1) -6.51	0	-1.0	310	-0.9	200		
		2) 0.0							
		1) -16.21	110	-9.0	710	-4.9	800		
		2) -9.7							
		1) -25.71	190	-10.0	1090	-8.0	1200		
		2) -19.2							
		1) -29.31	410	-15.0	1730	-7.8	2300		
		2) -22.8							
Speed (km/h)		1) 3 2) 30, 120	3, 30, 120	3, 30, 120	3				
UE/Mobile Station	Topology	Reference 0.5?	Reference 0.5?	Reference 0.5?	N/A				
	PAS	1) LOS on: Fixed AoA for LOS component, remaining power has 360 degree uniform PAS. 2) LOS off: PAS with a Lapacian distribution, RMS angle spread of 35 degrees per path	RMS angle spread of 35 degrees per path with a Lapacian distribution Or 360 degree uniform PAS.	RMS angle spread of 35 degrees per path with a Lapacian distribution	N/A				
	DoT (degrees)	0	22.5	-22.5	N/A				

Model		Case I	Case II	Case III	Case IV
	AoA (degrees)	22.5 (LOS component) 67.5 (all other paths)	67.5 (all paths)	22.5 (odd numbered paths), -67.5 (even numbered paths)	N/A
Node B/ Base Station	Topology	Reference: ULA with 0.5 λ -spacing or 4 λ -spacing or 10 λ -spacing			N/A
	PAS	Lapacian distribution with RMS angle spread of 2 degrees or 5 degrees, per path depending on AoA/AoD			N/A
	AoD/AoA (degrees)	50 $^\circ$ for 2 $^\circ$ RMS angle spread per path 20 $^\circ$ for 5 $^\circ$ RMS angle spread per path			N/A

1 Table 2-1. Summary of suggested SCM link level parameters for calibration purpose

2 *Designators correspond to channel models previously proposed in 3GPP and 3GPP2 a
3 groups.

4 **2.3 Spatial Parameters per Path**

5 Each resolvable path is characterized by its own spatial channel parameters (angle sp
6 angle of arrival, power azimuth spectrum). All paths are assumed independent.
7 assumptions apply to both the BS and the MS specific spatial parameters. The
8 assumptions are in effect only for the Link Level channel model.

9 **2.4 BS and MS Array Topologies**

10 The spatial channel model should allow any type of antenna configuration to be sel
11 although details of a given configuration must be shared to allow others to reproduce the
12 and verify the results.

13 Calibrating simulators at the link level requires a common set of assumptions includ
14 specific set of antenna topologies to define a baseline case. At the MS, the reference ele
15 spacing is 0.5 λ . At the BS, three values for reference element spacing are defined: 0.5 λ , 4 λ
16 10 λ .

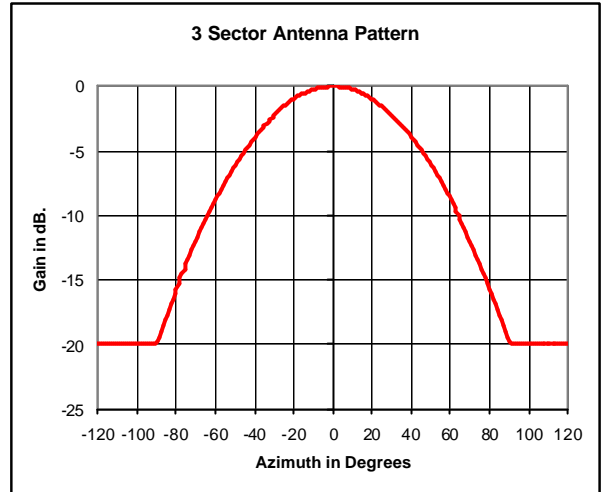
17 **2.5 Spatial Parameters for the BS**

18 2.5.1 BS Antenna Pattern

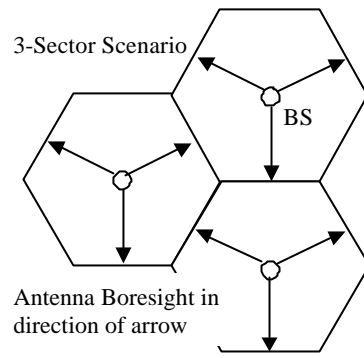
19 The 3-sector antenna pattern used for each sector, Reverse Link and Forward Link, is p
20 in **Figure 2-1** and is specified by

$$A(\theta) = \min\left\{12\frac{A_m}{\theta_{3dB}^2}, A_m\right\} \text{ where } \theta \in [180 - \theta_{3dB}, 180 + \theta_{3dB}]$$

θ is defined as the angle between the direction of interest and the boresight of the antenna. θ_{3dB} is the 3dB beamwidth in degrees, and A_m is the maximum attenuation. For a 3-sector scenario θ_{3dB} is 70°, A_m is 20dB, and the antenna boresight pointing direction is given in **Figure 2-2**. For a 6 sector scenario θ_{3dB} is 35°, A_m is 23dB, which results in the pattern shown in **Figure 2-3**, and the boresight pointing direction defined by **Figure 2-4**. boresight is defined to be the direction to which the antenna shows the maximum gain. The gain specified for the 3-sector 70° antenna is 14dBi. By reducing the beamwidth by half the corresponding gain will be 3dB higher resulting in 17dBi. The antenna pattern shown is targeted for diversity oriented implementations (i.e. large inter-element spacings) beamforming applications that require small spacings, alternative antenna designs may have been considered leading to a different antenna pattern.

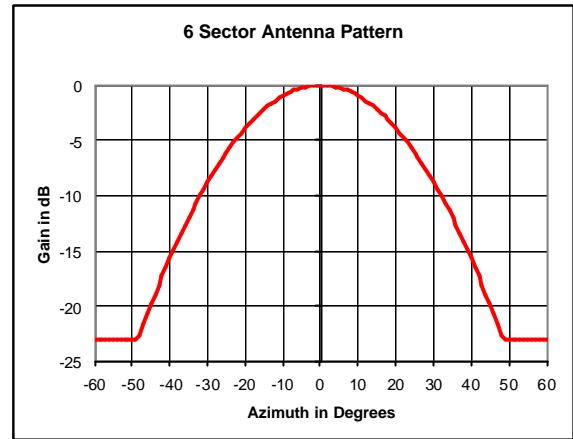


13
 14
 Figure 2-1. Antenna pattern for 3-sector cells



1
2
3

Figure 2-2. Boresight pointing direction for 3-sector cells



4
5
6

Figure 2-3. Antenna pattern for 6-sector cells

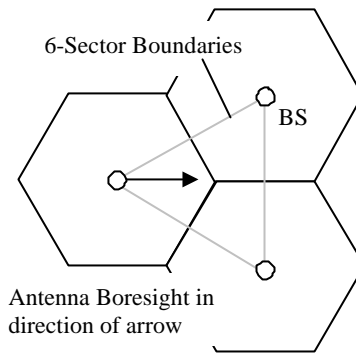


Figure 2-4. Boresight pointing direction for 6-sector cells

1
2

3 2.5.2 Per Path BS Angle Spread (AS)

4 The base station per path angle spread is defined as the root mean square (RMS) of angle
5 which an arriving path's power is received by the base station array. The individual
6 powers are defined in the temporal channel model described in Table 2-1. Two values
7 angle spread (each associated with a corresponding mean angle of arrival, AoA) are consid

- 8 - AS: 2 degrees at AoA 50 degrees
- 9 - AS: 5 degrees at AoA 20 degrees

10 It should be noted that attention should be paid when comparing the link level perform
11 between the two angle spread values since the BS antenna gain for the two corresponding
12 will be different. The BS antenna gain is applied to the path powers specified in Table 2-1

13 2.5.3 Per Path BS Angle of Arrival

14 The Angle of Arrival (AoA) or Angle of Departure (AoD) is defined to be the mean angle
15 which an arriving or departing path's power is received or transmitted by the BS array
16 respect to the boresite. The two values considered are:

- 17 - AoA: 50 degrees (associated with the RMS Angle Spread of 2 degrees)
- 18 - AoA: 20 degrees (associated with the RMS Angle Spread of 5 degrees)

19 2.5.4 Per Path BS Power Azimuth Spectrum

20 The Power Azimuth Spectrum (PAS) of a path arriving at the base station is assumed to
21 Laplacian distribution. For an incoming AOA $\bar{\theta}$ and RMS angle-spread σ , the BS per pat
22 value at an angle θ is given by:

23

24

$$P(\theta, \bar{\theta}, \sigma) = N_0 \exp\left\{-\frac{\sqrt{2} \sigma |\theta - \bar{\theta}|}{\sigma}\right\} G(\theta)$$

1 where both angles $\bar{\theta}$ and θ are given with respect to the boresight of the antenna element
 2 assumed that all antenna elements' orientations are aligned. Also, P is the average rec
 3 power and G is the numeric base station antenna gain described in Section 2.5.1 by

$$G(\theta) = 10^{0.1A(\theta)}$$

4
 5 Finally, N_0 is the normalization constant:

$$N_0^{-1} = \int_{-\pi/2}^{\pi/2} \exp\left\{-\frac{\sqrt{2}|\theta - \bar{\theta}|}{\sigma}\right\} G(\theta) d\theta$$

7 In the above equation, θ represents path components (sub-rays) of the path power arriv
 8 an incoming AoA $\bar{\theta}$. The distribution of these path components is TBD.

9 **2.6 Spatial Parameters for the MS**

10 2.6.1 MS Antenna Pattern

11 For each and every antenna element at the MS, the antenna pattern will be assumed
 12 directional with an antenna gain of -1 dBi.

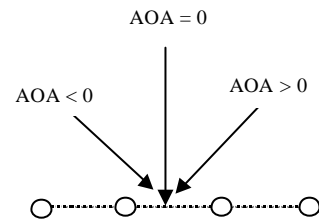
13 2.6.2 Per Path MS Angle Spread (AS)

14 The MS per path AS is defined as the root mean square (RMS) of angles of an incident p
 15 power at the MS array. Two values of the path's angle spread are considered:

- 16 - AS: 104 degrees (results from a uniform over 360 degree PAS),
- 17 - AS: 35 degrees for a Laplacian PAS with a certain path specific Angle of Arrival (Ao

18 2.6.3 Per Path MS Angle of Arrival

19 The per path Angle of Arrival (AOA) is defined as the mean of angles of an incident path's
 20 at the UE/Mobile Station array with respect to the broadside as shown **Figure 2-5**.



22 Figure 2-5. Angle of arrival orientation at the MS.

23 Three different per path AoA values at the MS are suggested for the cases of a non-u
 24 PAS, see Table 2-1 for details:

- 25 - AoA: -67.5 degrees (associated with an RMS Angle Spread of 35 degrees)
- 26 - AoA: +67.5 degrees (associated with an RMS Angle Spread of 35 degrees)

- 1 - AoA: +22.5 degrees (associated with an RMS Angle Spread of 35 degrees or
2 with an LOS component)

3 2.6.4 Per Path MS Power Azimuth Spectrum

4 The Laplacian distribution and the Uniform distribution are used to model the per path
5 Azimuth Spectrum (PAS) at the MS.

6 The Power Azimuth Spectrum (PAS) of a path arriving at the MS is modeled as ei
7 Laplacian distribution or a uniform over 360 degree distribution. Since an omni direction
8 antenna gain is assumed, the received per path PAS will remain either Laplacian or un
9 For an incoming AOA $\bar{\theta}$ and RMS angle -spread σ , the MS per path Laplacian PAS value
10 angle θ is given by:

$$11 \quad P(\theta, \bar{\theta}, \sigma) = N_o \exp\left\{-\frac{\sqrt{2}|\theta - \bar{\theta}|}{\sigma}\right\}$$

12 where both angles $\bar{\theta}$ and θ are given with respect to the boresight of the antenna element
13 assumed that all antenna elements' orientations are aligned. Also, P is the average rec
14 power and N_o is the normalization constant:

$$15 \quad N_o^{-1} = \int_{-\pi}^{\pi} \exp\left\{-\frac{\sqrt{2}|\theta - \bar{\theta}|}{\sigma}\right\} d\theta$$

16 In the above equation, σ represents path components (sub-rays) of the path power arriv
17 an incoming AoA $\bar{\theta}$. The distribution of these path components is TBD.

18 2.6.5 MS Direction of Travel

19 The mobile station direction of travel is defined with respect to the broadside of the n
20 antenna array as shown in **Figure 2-5**.

21 2.6.6 Per Path Doppler Spectrum

22 The per path Doppler Spectrum is defined as a function of the direction of travel and th
23 path PAS and AoA at the MS. This should correspond to the per path fading behavior for
24 the correlation-based or ray-based method.

25 2.7 Generation of Channel Model

26 The proponent can determine the model implementation. Examples of implementations in
27 correlation or ray-based techniques.

28 Outline of methodology, including doppler spectrum filter is required for correlation meth

29 2.8 Calibration and Reference Values

30 For the purpose of link level simulations, reference values of the average correlation are
31 below in **Table 2-2**. The reference values are provided for the calibration of the simu
32 software and to assist in the resolution of possible errors in the simulation me

1 implemented. Specifically, the average complex correlation and magnitude of the cor
 2 correlation is reported between BS antennas and between MS antennas. The spatial para
 3 values used are those defined already throughout Section 2.

4

	Antenna Spacing	AS (degrees)	AOA (degrees)	Correlation (magnitude)	Complex Correlation
BS	0.5 ?	5	20	0.9688	0.4743+0.844
	0.5 ?	2	50	0.9975	-0.7367+0.67
	4 ?	5	20	0.3224	-0.2144+0.24
	4 ?	2	50	0.8624	0.8025+0.315
	10 ?	5	20	0.0704	-0.0617+i0.0
	10 ?	2	50	0.5018	-0.2762-i0.41
MS	? /2	104	0	0.3042	-0.3042
	? /2	35	-67.5	0.7744	-0.6948-i0.3
	? /2	35	22.5	0.4399	0.0861+0.43
	? /2	35	67.5	0.7744	-0.6948+i0.3

5

Table 2-2. Reference correlation values.

6 3 SPATIAL CHANNEL MODEL FOR SIMULATIONS

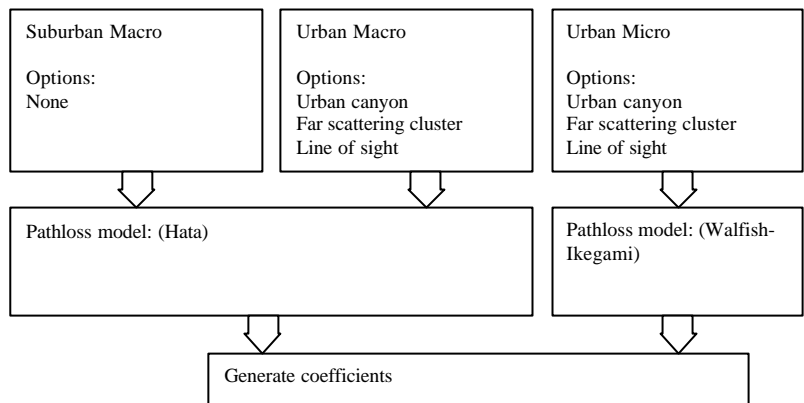
7 The spatial channel model for use in the system-level simulations is described in this sect

8 As opposed to link simulations which simply consider a single BS transmitting to a singl
 9 the system simulations typically consist of multiple cells, BSs, and MSs. Performance m
 10 such as throughput and delay are collected over D drops, where a "drop" is defined
 11 simulation run for a given number of cells, BSs, and MSs, over a specified number of fr
 12 During a drop, the channel undergoes fast fading according to the motion of the MSs. Ch
 13 state information is fed back from the MSs to the BSs, and the BSs use schedule
 14 determine which user(s) to transmit to. Typically, over a series of D drops, the cell layou
 15 locations of the BSs are fixed, but the locations of the MSs are randomly varied a
 16 beginning of each drop. To simplify the simulation, only a subset of BSs will actual
 17 simulated while the remaining BSs are assumed to transmit with full power. (Que
 18 remain about how to model interfering BS powers.)

19 The goal of this section is to define the methodology and parameters for generating the s
 20 and temporal channel coefficients between a given base and mobile for use in system
 21 simulations. For an S element BS array and a U element MS array, the channel coefficient
 22 one of N multipath components (note that these components are not necessarily
 23 resolvable, meaning that the time difference between successive paths may be less than
 24 period) are given by an S -by- U matrix of complex amplitudes. We denote the channel r
 25 for the n th multipath component ($n = 1, \dots, N$) as $\mathbf{H}_n(t)$. It is a function of time t becau

1 complex amplitudes are undergoing fast fading governed by the movement of the MS
 2 overall procedure for generating the channel matrices consists of three basic steps:
 3 1. Specify an environment, either suburban macro, urban macro, or urban micro (S
 4 3.2).
 5 2. Obtain the parameters to be used in simulations, associated with that environment (S
 6 3.3).
 7 3. Generate the channel coefficients based on the parameters (Section 3.4).
 8 Sections 3.2, 3.3, and 3.4 give the details for the general procedure. **Figure 3-1** below pr
 9 a roadmap for generating the channel coefficients. (This diagram should be greatly exp
 10 and should show which section numbers each of the items is discussed.) Section 3.5 con
 11 options for modifying the general procedure. Section 3.6 describes the procedure for gene
 12 correlated log normal user parameters used in Section 3.3. Section 3.7 describes the m
 13 for accounting for intercell interference. Section 3.8 presents calibration results.

14



15

16

Figure 3-1. Channel model overview for simulations

17 **3.1 General definitions, parameters, and assumptions**

18 The received signal at the MS consists of N time-delayed multipath replicas of the transr
 19 signal. These N paths are defined by powers and delays and are chosen randomly accord
 20 the channel generation procedure. Each path consists of M subpaths.

21

22 **Figure 3-2** shows the angular parameters used in the model. The following definitions are
 23 used:

- 24 θ_{BS} BS antenna array orientation, defined as the difference between the broadside of
 25 BS array and the absolute North (N) reference direction.
- 26 θ_{BS} LOS AoD direction between the BS and MS, with respect to the broadside of th
 27 array.
- 28 $\theta_{n,AoD}$ AoD for the n th ($n = 1 \dots N$) path with respect to the LOS AoD θ_0 .

- 1 $\varphi_{n,m,AoD}$ Offset for the m th ($m = 1 \dots M$) subpath of the n th path with respect to $\varphi_{n,AoD}$.
- 2 $\varphi_{n,m,AoD}$ Absolute AoD for the m th ($m = 1 \dots M$) subpath of the n th path at the BS with re
- 3 to the BS broadside.
- 4 φ_{MS} MS antenna array orientation, defined as the difference between the broadside
- 5 MS array and the absolute North reference direction.
- 6 φ_{MS}^{LOS} Angle between the BS-MS LOS and the MS broadside.
- 7 $\varphi_{n,AoA}$ AoA for the n th ($n = 1 \dots N$) path with respect to the LOS AoA $\varphi_{0,MS}$.
- 8 $\varphi_{n,m,AoA}$ Offset for the m th ($m = 1 \dots M$) subpath of the n th path with respect to $\varphi_{n,AoA}$.
- 9 $\varphi_{n,m,AoA}$ Absolute AoA for the m th ($m = 1 \dots M$) subpath of the n th path at the BS with re
- 10 to the BS broadside.
- 11 \mathbf{v} MS velocity vector.
- 12 φ_v Angle of the velocity vector with respect to the MS broadside: $\varphi_v = \arg(\mathbf{v})$.

13 The angles shown in Figure 1 that are measured in a clockwise direction are assumed to
 14 negative in value.

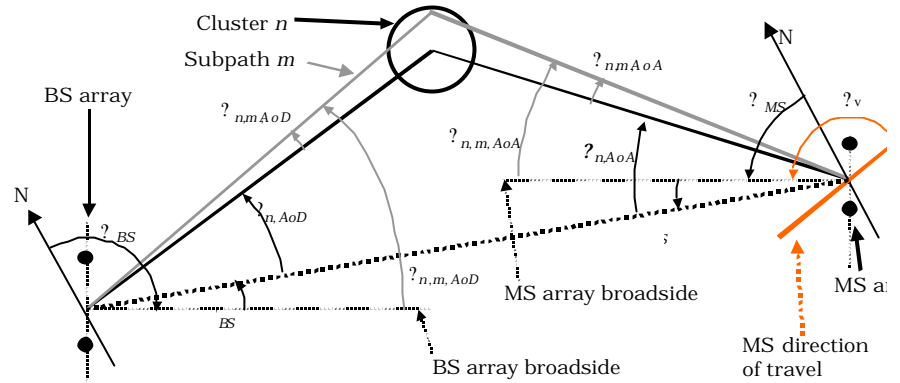


Figure 3-2. BS and MS angle parameters

17 For system level simulation purposes, the fast fading per-path will be evolved in time, altho
 18 bulk parameters including angle spread, delay spread, log normal shadowing, and MS lo
 19 will remain fixed during the evaluation of the given MS.

20 The following are general assumptions made for all simulations, independent of environm

- 21 1. Uplink-Downlink Reciprocity: The AoD/AoA values are identical between the uplink
- 22 downlink.
- 23 2. Random path phases between UL, DL are uncorrelated.
- 24 3. Mobile-to-mobile shadowing is uncorrelated.
- 25 4. The spatial channel model should allow any type of antenna configuration to be sel
- 26 although details of a given configuration must be shared to allow others to reprodu

1 model and verify the results. It is intended that the spatial channel model be capa
 2 operating on any given antenna array configuration. In order to compare algorit
 3 reference antenna configurations based on uniform linear array configurations with (
 4 and 10 wavelength inter-element spacing will be used.

5 **3.2 Environments**

6 We consider the following three environments.

- 7 1. Suburban macrocell (approximately 3Km distance BS to BS)
- 8 2. Urban macrocell (approximately 3Km distance BS to BS)
- 9 3. Urban microcell (less than 1Km distance BS to BS)

10 The characteristics of the macro cell environments assume that BS antennas are above r
 11 height. For the urban microcell scenario, we assume the BS antenna is at rooftop height.
 12 3-1 describes the parameters used in each of the environments.

13

Channel Scenario	Suburban Macro	Urban Macro	Urban Micro
Number of paths (N)	6	6	6
Number of sub-paths (M) per path	20	20	20
Mean composite AS at BS	$E(\gamma_{AS})=5^0$	$E(\gamma_{AS})=8^0, 15^0$	NLOS: $E(\gamma_{AS})=1$
r_{DS} ($\gamma_{delays}/\gamma_{DS}$)	1.4	1.7	N/A
r_{AS} ($\gamma_{AoD}/\gamma_{PAS}$)	1.2	1.3	N/A
Composite AS at BS as a lognormal RV when simulating with 6 paths $\gamma_{AS} \sim 10^{\sum_{i=1}^6 x_i}$, $x_i \sim \mathcal{N}(0,1)$	$\gamma_{AS} = 0.69$ $\gamma_{AS} = 0.13$	$8^0 \gamma_{AS} = 0.810$ $\gamma_{AS} = 0.3295$ $15^0 \gamma_{AS} = 1.18$ $\gamma_{AS} = 0.210$	N/A
Per path AS at BS (Fixed)	2 deg	2 deg	5 deg (LOS and
BS Per path AoD Distribution st dev	$N(0, \sigma_{AoD}^2)$, where $\sigma_{AoD} = r_{AS} \gamma_{AS}$	$N(0, \sigma_{AoD}^2)$, where $\sigma_{AoD} = r_{AS} \gamma_{AS}$	$U(-40deg, 40deg)$
Mean of RMS composite AS at MS	$E(\gamma_{AS, comp, UE})=72^0$	$E(\gamma_{AS, comp, UE})=72^0$	$E(\gamma_{AS, comp, UE})=72^0$
Per path AS at MS (fixed)	35^0	35^0	35^0
MS Per path AoA Distribution	$N(0, \sigma_{AoA}^2 (P_r))$	$N(0, \sigma_{AoA}^2 (P_r))$	$N(0, \sigma_{AoA}^2 (P_r))$
Mean total RMS Delay Spread	$E(\gamma_{DS})=0.17 \gamma_s$	$E(\gamma_{DS})=0.65 \gamma_s$	N/A

Distribution for path delays			$U(0, 1.2?)s$
Narrowband composite delay spread as a lognormal RV when simulating with 6 paths $\sigma_{DS} = 10^{\frac{1}{2} \ln(\sigma_{DS}^2)}$, $x \sim \mathcal{N}(0,1)$	$\mu_{DS} = -6.80$ $\sigma_{DS} = 0.288$	$\mu_{DS} = -6.18$ $\sigma_{DS} = 0.18$	N/A
Lognormal shadowing standard deviation	8dB	8dB	NLOS: 10dB LOS: 4dB
Pathloss model (dB), d is in meters	NLOS and LOS: $28.6 + 35\log_{10}(d)$	NLOS and LOS: $28.6 + 35\log_{10}(d)$	NLOS: $36 + 38\log_{10}(d)$ LOS: $30.6 + 26\log_{10}(d)$

Table 3-1. Environment parameters

- The following are assumptions made for the *suburban macrocell* and *urban macrocell* environments.
- The macrocell pathloss from 3GPP2 evaluation methodology will be used, based on modified Hata urban propagation model at 1.9 GHz carrier frequency (COST 231). Assuming the BS antenna height is 32m, and the MS antenna height is 1.5m, the pathloss is $28.6 + 35\log_{10}(d)$ dB, where d is distance between the BS and MS in meters. d is at least 35m.
 - Antenna patterns at the BS are the same as those used in the link simulations given in Section 2.5.1.
 - Site-to-site LN correlation is $\rho = 0.5$. This parameter is used in Section 3.6.2.
- The following are assumptions made for the *microcell* environment.
- Antenna patterns at the BS are the same as those used in the link simulations given in Section 2.5.1.
 - Site-to-site correlation follows the macrocell model ($\rho = 0.5$).
 - The hexagonal cell repeats will be the assumed layout.
- For the microcell NLOS environment, a Walfish-Ikegami model is used with the following parameters: BS antenna height 12.5m, building to building distance 50m, street width 10m, MS antenna height 1.5m, orientation 30deg for all paths, frequency 2GHz. The resulting pathloss equation is $36 + 38\log_{10}(d)$, where d is in meters. A bulk log normal shadowing applying to all paths has a standard deviation of 10dB.
- For the microcell LOS environment, a Walfish-Ikegami street canyon model is used. The resulting pathloss is $30.6 + 26\log_{10}(d)$, where d is in meters. A bulk log normal shadowing applying to all paths has a standard deviation of 4dB.

3.3 Generating User Parameters

For a given scenario and set of parameters given by a column of Table 3-1, realizations of user's parameters such as the path delays, powers, and subpath angles of departure arrival can be derived using the procedure described here in Section 3.3. In particular, Section 3.3.1 gives the steps for the urban macrocell and suburban macrocell environments. Section 3.3.2 gives the steps for the urban microcell environments.

3.3.1 Generating user parameters for urban macrocell and suburban macrocell environments

Step 1: Choose either an urban macrocell or suburban macrocell environment.

Step 2: Determine various distance and orientation parameters. The placement of the MS with respect to each BS is to be determined according to the cell layout. From this placement the distance between the MS and the BS (d) and the LOS directions with respect to the BS are (θ_{BS} and θ_{MS} , respectively) can be determined. The MS antenna array orientations (θ_{MS}) are i.i.d., drawn from a uniform 0 to 360 degree distribution. The MS velocity vector \mathbf{v} is drawn from a uniform 0 to 360 degree distribution. The MS velocity magnitude $\|\mathbf{v}\|$ is drawn according to a velocity distribution (to be determined) and the direction is drawn from a uniform 0 to 360 degree distribution.

Step 3: Determine the DS, AS, and LN. These variables, given respectively by τ_{DS} , τ_{AS} , and τ_{LN} , are generated as described in Section 3.6 below. Note that $10^{\tau_{DS}}$ is in units of seconds so that the narrowband composite delay spread τ_{DS} is in units of seconds. Note also that we have dropped the BS indices used in Section 3.6.1 to simplify notation.

Step 4: Determine random delays for each of the N multipath components. For macrocell environments, $N=6$ as given in Table 3.1. Generate random variables τ'_1, \dots, τ'_N according to

$$\tau'_n = \tau_{DS} \tau_{DS} \log z_n \quad n = 1, \dots, N$$

where z_n ($n = 1, \dots, N$) are i.i.d. random variables with uniform distribution $U(0,1)$, τ_{DS} is given in Table 3-1, and τ_{DS} is derived in Step 2 above. These variables are ordered so that $\tau'_{(N)} \geq \tau'_{(N-1)} \geq \dots \geq \tau'_{(1)}$ and the minimum of these is subtracted from all so that the first delay is always zero. The delays are quantized in time to the nearest 1/16th chip interval. Then the delays are given by:

$$\tau_n = \frac{T_c}{16} \left\lfloor \frac{\tau'_{(n)} - \tau'_{(1)}}{T_c/16} \right\rfloor + 0.5 \frac{T_c}{16} \quad n = 1, \dots, N,$$

where $\text{floor}(x)$ is the integer part of x , and T_c is the chip interval ($T_c = 1/3.84 \times 10^6$ sec for 3GPP1 and $T_c = 1/1.2288 \times 10^6$ sec for 3GPP2). Then the 6 delays are given by:

$$\tau_n = \tau'_{(n)} - \tau'_{(1)}, \quad n = 1, \dots, N.$$

Note that these delays are ordered so that $\tau_N \geq \tau_5 \geq \dots \geq \tau_1 \geq 0$. (See notes 1 and 2 at the end of Section 3.3.1.) Quantization to 1/16 chip is the default value. For special implementations, possibly higher quantization values may be used if needed.

Step 5: Determine random average powers for each of the N multipath components. The unnormalized powers are given by

$$P_n = e^{-\frac{(r_{DS}^2 \gamma_{(n)}^2 \gamma_{(1)}^2)}{r_{DS}^2 \gamma_{DS}^2}} 10^{\gamma_n}, n = 1, \dots, 6$$

where γ_n ($n = 1, \dots, 6$) are i.i.d. Gaussian random variables with variance $\gamma_{RND}^2 = 3$ dB, which is a shadowing randomization effect on the per-path powers. Note that the powers are determined using the unquantized channel delays. Average powers are normalized so that total average power for all six paths is equal to one:

$$P_n = \frac{P_n'}{\sum_{n=1}^6 P_n'}$$

(See note 3 at the end of Section 3.3.1.)

Step 6: Determine AoDs for each of the N multipath components. First generate i.i.d. zero Gaussian random variables:

$$\gamma_n' \sim \mathcal{N}(0, \gamma_{AoD}^2), \quad n = 1, \dots, N,$$

where $\gamma_{AoD} = r_{AS} \gamma_{AS}$. The value r_{AS} is given in Table 3-1 and depends on whether the urban or suburban macrocell environment is chosen. The angle spread γ_{AS} is generated in Step 3. The variables are given in degrees. They are ordered in increasing absolute value so that $|\gamma_{(1)}'| \geq |\gamma_{(2)}'| \geq \dots \geq |\gamma_{(N)}'|$. The AoDs $\gamma_{n,AoD}$, $n = 1, \dots, N$ are assigned to the ordered variables so that $\gamma_{n,AoD} = \gamma_{(n)}'$, $n = 1, \dots, N$. (See note 4 at the end of Section 3.3.1.)

Step 7: Associate the multipath delays with AoDs. The n th delay τ_n generated in Step 5 is associated with the n th AoD $\gamma_{n,AoD}$ generated in Step 6.

Step 8: Determine the powers, phases, and offset AoDs of the $M = 20$ sub-paths for each of the N paths at the BS. All 20 sub-paths associated with the n th path have identical powers (where P_n is from Step 5) and i.i.d. phases $\gamma_{n,m}$ drawn from a uniform 0 to 360 degree distribution. The relative offset of the m th subpath ($m = 1, \dots, M$) $\gamma_{n,m,AoD}$ is a fixed value in Table 3-2. For example, for the urban and suburban macrocell cases, the offsets for the first and second sub-paths are respectively $\gamma_{n,1,AoD} = 0.0894$ and $\gamma_{n,2,AoD} = -0.0894$ degrees. The offsets are chosen to result in the desired per path angle spread (2 degrees for the macrocell environments, and 5 degrees for the microcell environment).

Step 9: Determine the AoAs for each of the multipath components. The AoAs are i.i.d. Gaussian random variables

$$\gamma_{n,AoA} \sim \mathcal{N}(0, \gamma_{nAoA}^2), \quad n = 1, \dots, N,$$

where $\gamma_{nAoA} = 104.12 \sqrt{1 - \exp[-0.2175(10 \log_{10}(P_n))]}$ and P_n is the relative power of the n th path from Step 5.

Step 10: Determine the offset AoAs at the UE of the $M = 20$ sub-paths for each of the N paths at the MS. As in Step 8 for the AoD offsets, the relative offset of the m th subpath ($m = 1,$

1 $\theta_{n,m,AoA}$ is a fixed value given in Table 3-2. These offsets are chosen to result in the desired
2 path angle spread of 35 degrees.

3 **Step 11:** Associate the BS and MS paths and sub-paths. The n th BS path (defined by its
4 θ_n , power P_n , and AoD $\theta_{n,AoD}$) is associated with the n th MS path (defined by its AoA θ_n).
5 For the n th path pair, randomly pair each of the M BS sub-paths (defined by its offset $\theta_{n,m}$
6 and phase $\theta_{n,m}$) with a MS sub-path (defined by its offset $\theta_{n,m,AoA}$). To simplify the notation
7 we renumber the M MS sub-path offsets with their newly associated BS sub-path. In other
8 words, if the first ($m = 1$) BS sub-path is randomly paired with the 10th ($m = 10$) MS sub-
9 path we re-associate $\theta_{n,1,AoA}$ (after pairing) with $\theta_{n,10,AoA}$ (before pairing).

10 **Step 12:** Determine the antenna gains of the BS and MS sub-paths as a function of
11 respective sub-path AoDs and AoAs. For the n th path, the AoD of the m th sub-path
12 (with respect to the BS antenna array broadside) is

$$13 \theta_{n,m,AoD} = \theta_{BS} + \theta_{n,AoD} + \theta_{n,m,AoD}.$$

14 Similarly, the AoA of the m th sub-path for the n th path (with respect to the MS antenna
15 broadside) is

$$16 \theta_{n,m,AoA} = \theta_{MS} + \theta_{n,AoA} + \theta_{n,m,AoA}.$$

17 The antenna gains are dependent on these sub-path AoDs and AoAs. For the BS and MS,
18 the gains are given respectively as $G_{BS}(\theta_{n,m,AoD})$ and $G_{MS}(\theta_{n,m,AoA})$.

19 Notes:

20 Note 1: In the development of the Spatial Channel Model, care was taken to include
21 statistical relationships between Angles and Powers, as well as Delays and Powers. This was
22 done using the proportionality factors $\rho_{DS} = \theta_{delays}/\theta_{DS}$ and $\rho_{AS} = \theta_{AoD}/\theta_{PAS}$ that were based
23 on measurements.)

24 Note 2: While there is some evidence that delay spread may depend on distance between
25 transmitter and receiver, the effect is considered to be minor (compared to other dependencies
26 DS-AS, DS-LN.). Various inputs based on multiple data sets indicate that the trend of DS
27 to be either slightly positive or negative, and may sometimes be relatively flat with distance.
28 For these reasons and also for simplicity, a distance dependence on DS is not modeled.

29 Note 3: The equations presented here for the power of the n th path are based on an
30 average delay envelope which is the average behavior of the power-delay profile. Defining the power
31 to reproduce the average behavior limits the dynamic range of the result and does not reproduce
32 the expected randomness from trial to trial. The randomizing noise θ_n is used to vary
33 the powers with respect to the average envelope to reproduce the variations experienced in
34 the actual channel. This parameter is also necessary to produce a dynamic range comparable
35 to measurements.

36 Note 4: The quantity ρ_{AS} describes the distribution of powers in angle and $\rho_{AS} = \theta_{AoD}/\theta_{AS}$ is
37 the spread of angles to the power weighted angle spread. Higher values of ρ_{AS} correspond to
38 power being concentrated in a small AoD or a small number of paths that are closely spaced
39 in angle.

1 3.3.2 Generating user parameters for urban microcell environments

2 Urban microcell environments differ from the macrocell environments in that the indiv
3 multipaths are independently shadowed. Also, only $N = 3$ (instead of 6) paths are mo
4 because of the reduced delay spread in microcells. We list the entire procedure but
5 describe the details of the steps that differ from the corresponding step of the mac
6 procedure.

7 **Step 1:** Choose the urban microcell environment.

8 **Step 2:** Determine various distance and orientation parameters.

9 **Step 3:** Determine the DS, AS, and LN.

10 **Step 4:** Determine the random delays for each of the N multipath components. For the mic
11 environment, $N = 6$. The delays $\tau_n, n = 1, \dots, N$ are i.i.d. random variables drawn fr
12 uniform distribution from 0 to 1.2 τ_s .

13 **Step 5:** Determine random average powers for each of the N multipath components. Thi
14 consists of $N=6$ distinct paths that are uniformly distributed between 0 and 1.2 τ_s . The p
15 for each path are exponentially decaying in time with the addition of a lognormal random
16 which is independent of the path delay:

$$17 \quad P_n = 10^{z_n} \tau_n^{-\alpha}$$

18 where τ_n is given in units of microseconds, and z_n ($n = 1, \dots, N$) are i.i.d. zero mean Gau
19 random variables with variance of $(3\text{dB})^2$. The lognormal variation of each path produc
20 variation seen in the path powers, and a separate log normal shadowing value is appl
21 common to all paths.

22 **Step 6:** Determine AoDs for each of the N multipath components. The AoDs (with respect
23 LOS direction) are i.i.d. random variables drawn from a uniform distribution over -40 t
24 degrees:

$$25 \quad \theta_{nAoD} \sim U(-40, 40), \quad n = 1, \dots, N,$$

26 Associate the AoD of the n th path θ_{nAoD} with the power of the n th path P_n . Note unlik
27 macrocell environment, the AoDs do not need to be sorted before being assigned to a
28 power.

29 **Step 7:** Associate the multipath delays with AoDs.

30 **Step 8:** Determine the powers, phases, and offset AoDs of the $M = 20$ sub-paths for each o
31 paths at the BS. The offsets are given in Table 3-2, and the resulting per path AS is 5 de
32 instead of 2 degrees for the macrocell case.

33 **Step 9:** Determine the AoAs for each of the multipath components. The AoAs are i.i.d Gau
34 random variables

$$35 \quad \theta_{nAoA} \sim \mathcal{N}(0, \sigma_{nAoA}^2), \quad n = 1, \dots, N,$$

36 where $\sigma_{nAoA}^2 = 104.12 \left[1 - \exp\left\{-0.265 \left| 10 \log_{10} \left(\frac{P_n}{P_{nAoA}} \right) \right|^2 \right\} \right]$ and P_n is the relative power of the n th
37 from Step 5.

38 **Step 10:** Determine the offset AoAs of the $M = 20$ sub-paths for each of the N paths at the M

1 **Step 11:** Associate the BS and MS paths and sub-paths.

2 **Step 12:** Determine the antenna gains of the BS and MS sub-paths as a function of
 3 respective sub-path AoDs and AoAs.

4

Sub-path # (<i>m</i>)	Offset for a 2 deg AS at BS (Macrocell) $\theta_{n,m,AoD}$ (degrees)	Offset for a 5 deg AS at BS (Microcell) $\theta_{n,m,AoD}$ (degrees)	Offset for a 35 deg AS at MS $\theta_{n,m,AoA}$ (degrees)
1, 2	0.0894	0.2236	1.5649
3, 4	0.2826	0.7064	4.9447
5, 6	0.4984	1.2461	8.7224
7, 8	0.7431	1.8578	13.0045
9, 10	1.0257	2.5642	17.9492
11, 12	1.3594	3.3986	23.7899
13, 14	1.7688	4.4220	30.9538
15, 16	2.2961	5.7403	40.1824
17, 18	3.0389	7.5974	53.1816
19, 20	4.3101	10.7753	75.4274

5

Table 3-2. Sub-path AoD and AoA offsets

6 The values in Table 3-2 are selected to produce a biased standard deviation equal to 2.5
 7 35 degrees, which is equivalent to the per-path power weighted azimuth spread for equal
 8 sub-paths.

9 **3.4 Generating channel coefficients**

10 Given the user parameters generated in Section 3.3, we use them to generate the ch
 11 coefficients. For an *S* element BS array and a *U* element MS array, the channel coefficient
 12 one of *N* multipath components are given by an *S*-by-*U* matrix of complex amplitude
 13 denote the channel matrix for the *n*th multipath component (*n* = 1,...,*N*) as $\mathbf{H}_n(t)$. The
 14 component (*s* = 1,...,*S*; *u* = 1,...,*U*) of $\mathbf{H}_n(t)$ is given by

15
$$h_{s,u,n}(t) = \sqrt{\frac{P_n}{M}} \sum_{m=1}^M \frac{\sqrt{G_{BS}(\theta_{n,m,AoD})} \exp(jk d_s \sin(\theta_{n,m,AoD}))}{\sqrt{G_{MS}(\theta_{n,m,AoA})} \exp(jk d_u \sin(\theta_{n,m,AoA}))} \exp(jk \|\mathbf{v}\| \cos(\theta_{n,m,AoA}))$$

16 where

17 P_n is the power of the *n*th path (Step 5).

18 *M* is the number of subpaths per path.

19 $\theta_{n,m,AoD}$ is the the AoD for the *m*th subpath of the *n*th path (Step 12).

- 1 $\theta_{n,m,AoA}$ is the the AoA for the m th subpath of the n th path (Step 12).
- 2 $G_{BS}(\theta_{n,m,AoD})$ is the BS antenna array gain (Step 12).
- 3 $G_{MS}(\theta_{n,m,AoA})$ is the MS antenna array gain (Step 12).
- 4 j is the square root of -1.
- 5 k is the wave number $2\pi/\lambda$ where λ is the carrier wavelength in meters.
- 6 d_s is the distance in meters from BS antenna element s from the reference antenna. For the reference antenna $s = 1$, $d_1=0$.
- 7
- 8 d_u is the distance in meters from MS antenna element u from the reference antenna. For the reference antenna $u = 1$, $d_1=0$.
- 9
- 10 $\phi_{n,m}$ is the phase of the m th subpath of the n th path (Step 8).
- 11 $\|\mathbf{v}\|$ is the magnitude of the MS velocity vector (Step 2).
- 12 θ_v is the angle of the MS velocity vector (Step 2).

13 3.5 Optional system simulation features

14 3.5.1 Polarized arrays

15 Practical antennas on handheld devices require spacings much less than $\lambda/2$. Polarized antennas are likely to be the primary way to implement multiple antennas. A cross-polar model is therefore included here.

18 A method of describing polarized antennas is presented, which is compatible with the procedure given in section 3.3. The following steps extend the original 12 to account for additional polarized components. Each element of the S element BS array and U element array consists of cross-polarized elements.

- 22 - **Step 13:** *Generate additional cross-polarized subpaths.* For each of the 6 paths of S generate an addition M subpaths at the MS and M subpaths at the BS to represent portion of each signal that leaks into the cross-polarized antenna orientation due to scattering.
- 26 - **Step 14:** *Set subpath AoDs and AoAs.* Set the AoD and AoA of each subpath in S equal to that of the corresponding subpath of the co-polarized antenna orientation. (Orthogonal sub-rays arrive/depart at common angles.)
- 29 - **Step 15:** *Generate phase offsets for the cross-polarized elements.* We define $\theta_{n,m}^{(x,y)}$ to be the phase offset of the m th subpath of the n th path between the x component (e.g. either horizontal h or vertical v) of the BS element and the y component (e.g. either the horizontal or vertical v) of the MS element. Set $\theta_{n,m}^{(x,x)}$ to be $\theta_{n,m}$ generated in Step 8 of Section 3.3. Generate $\theta_{n,m}^{(x,y)}$, $\theta_{n,m}^{(y,x)}$, and $\theta_{n,m}^{(y,y)}$ as i.i.d random variables drawn from a uniform 0 to 360 degree distribution. (x and y can alternatively represent the co-polarized and cross-polar orientations.)

- 1 - **Step 16:** Decompose each of the co-polarized and cross-polarized sub-rays into vertical and horizontal components based on the co-polarized and cross-polarized orientations.
- 2
- 3 - **Step 17:** The power P2 of each ray in the cross-polarized orientation is set relative to the power P1 of each ray in the co-polarized orientation according to an XPD ratio, defined as XPD= P1/P2.
- 4
- 5
- 6 - For urban macrocells: $P2 = P1 - A - B \cdot N(0,1)$, where $A=0.34$ *(mean relative path power loss in dB), and $B=5.5$ dB is the standard deviation of the XPD variation.
- 7
- 8 - For urban microcells: $P2 = P1 - A - B \cdot N(0,1)$, where $A=8$ dB, and $B=8$ dB is the standard deviation of the XPD variation.
- 9
- 10 - **Step 18:** At the receive antennas, decompose each of the vertical and horizontal components into components that are co-polarized with the receive antennas and sum the components.
- 11
- 12 The fading behavior between the cross pol elements will be a function of the per-ray spreading rate and the Doppler. The fading between orthogonal polarizations has been observed to be independent and therefore the sub-rays phases are chosen randomly. The propagation characteristics of V-to-V paths are assumed to be equivalent to the propagation characteristics of H-to-H paths.
- 13
- 14
- 15 The polarization model can be illustrated by a matrix describing the propagation of and interaction between horizontal and vertical amplitude of each sub-path. The resulting channel realization is:
- 16
- 17
- 18
- 19

$$h_{s,u,n}(t) = \frac{1}{M} \sum_{m=1}^M \sqrt{\frac{P_n}{G_{BS}^{(v)}(\theta_{n,m,AoD})}} \exp\{j\phi_{n,m}^{(v,v)}\} \sqrt{r_n} \exp\{j\phi_{n,m}^{(h,v)}\} \sqrt{\frac{G_{MS}^{(v)}(\theta_{n,m,AoD})}{G_{MS}^{(h)}(\theta_{n,m,AoD})}} \exp\{jkd_s \sin(\theta_{n,m,AoD})\} \exp\{jkd_u \sin(\theta_{n,m,AoA})\} \exp\{jk\|\mathbf{v}\| \cos(\theta_{n,m,AoA} - \theta_v) t\}$$

21 where:

22 $G_{BS}^{(v)}(\theta_{n,m,AoD})$ is the BS antenna array gain for the vertically polarized component.

23 $G_{BS}^{(h)}(\theta_{n,m,AoD})$ is the BS antenna array gain for the horizontally polarized component.

24 $G_{MS}^{(v)}(\theta_{n,m,AoD})$ is the MS antenna array gain for the vertically polarized component.

25 $G_{MS}^{(h)}(\theta_{n,m,AoD})$ is the MS antenna array gain for the horizontally polarized component.

26 r_n is the average power ratio of waves of the n th path leaving the BS in the vertical direction and arriving at the MS in the horizontal direction (v-h) to those leaving in the vertical direction and arriving in the vertical direction (v-v). By symmetry, the power ratio of the opposite process (h-v over vv) is the same.

27

28

29

30 $\phi_{n,m}^{(h,h)}$ phase offset of the m th subpath of the n th path between the x component of the horizontal h or vertical v of the BS element and the y component (either horizontal h or vertical v) of the MS element.

31

32

33 The other variables are described in Section 3.4.

1

2 The 2x2 matrix represents the scattering phases and amplitudes of a plane wave leaving
 3 UE with a given angle and polarization and arriving Node B with another direction
 4 polarization. r_n is the average power ratio of waves leaving the UE in the vertical direction
 5 arriving at Node B in the horizontal direction (v-h) to those arriving at Node B in the vertical
 6 direction (v-v). By symmetry the power ratio of the opposite process (h-v over v-v) is chosen
 7 to be the same. Note that: $r_n = 1/XPD$; for the macrocell model, the XPD is dependent on the
 8 index; for the microcell model, the XPD is independent of path index.

9 Expression (2) assumes a random pairing of the of the sub-paths from the MS and BS
 10 random orientation of the MS (UE) array affects the value of the angle $\theta_{n,m,AoA}$ of each
 11 path.

12 If for example, vertically polarized antennas are used only at both NodeB and UE the
 13 antenna responses become $\begin{bmatrix} 1 \\ 0 \end{bmatrix}$ and expression (2) becomes identical to (1). For an ideal

14 antenna at the NodeB tilted with respect to the z-axis at θ degrees the above vector becomes
 15 $\begin{bmatrix} \cos(\theta) \\ \sin(\theta)\cos(\theta_{n,m,AoA}) \end{bmatrix}$.

16 The elevation spectrum is not modeled.

17 3.5.2 Far scatterer clusters

18 The Far scatterer cluster model is switch selectable. It represents the bad-urban case
 19 additional clusters are seen in the environment. This model is limited to use with the
 20 macro-cell where the first cluster will be the primary cluster and the second will be the
 21 scattering cluster (FSC). When the model is active, it will have the following characteristics:

- 22 1. There is a reduction in the number of paths in the primary cluster from $N = 6$ to $N = 4$
 23 the far scattering cluster then having $N = 2$. Thus the total number of paths will stay
 24 the same, now $N = 4 + 2$. This is a modification to the SCM channel generation procedure
 25 section 3.3.
- 26 2. FSCs will lie only outside a 500m radius from the BS/NodeB.
- 27 3. The FSCs will only be modeled for the serving cell, with 3 independent FSCs in the
 28 uniformly applied to the area of the cell outside the minimum radius.
- 29 4. The model statistics of the two clusters are identical (cluster DS, AS, PDF
 30 independently drawn. The FSC also has independent shadowing per path with a site-
 31 correlation of 50%.
- 32 5. The FSC is attenuated by 1dB/microsec delay with respect to the 1st cluster with a
 33 maximum. The excess delay will be defined as the difference in propagation time between
 34 the BS-MS LOS distance, and the BS-FSC-MS distance.
- 35 6. The FSC is modeled within the serving cell only and dropped following a uniform
 36 distribution.

1 The following method will be used to set the path powers: Draw the N=4 path powers from
 2 channel generation procedure in section 3.3, then draw a separate set of N=2 path powers from
 3 the same procedure. The two groups are kept separate and un-normalized. Now the
 4 based attenuation is applied to the group of N=2 paths, and the N=6 total paths are normalized
 5 to unity power after accounting for the bulk log normal shadowing per cluster including site
 6 site correlation

7 3.5.3 Line of sight

8 The Line-of-sight (LOS) model is an option that is switch selectable. It can be selected for
 9 micro cases. LOS modeling will not be defined for the suburban or urban cases. Its use is
 10 following description when this function is selected.

11 For the NLOS case, the Rice factor is set to 0, thus the fading is determined by the combination
 12 of sub-rays as described in section 3.3 of the model.

13 For the LOS case, the Rice factor K is based on a simplified version of [Foster 1994]: $K = 0.03 \cdot d$ (dB) where d is the distance between MS and BS in meters.

15 The probability for LOS or NLOS depends on various environmental factors, including city
 16 street canyons, and distance. For simplicity, the probability of LOS is defined to be unity at
 17 zero distance, and decreases linearly until a cutoff point at $d=300m$, where the LOS probability
 18 is zero.

$$19 \quad P(LOS) = \begin{cases} (300 - d)/300, & 0 \leq d \leq 300m \\ 0, & d > 300m \end{cases}$$

20 The K-factor, propagation slope, and shadow fading standard deviation will all be chosen
 21 on the results of selecting the path to be LOS or NLOS.

22 The K-factor will be formed by adding a direct component (sine wave) at the average angle of
 23 arrival (AoA) of the path such that the ratio of the power assigned to the direct component to the
 24 power assigned to the 6 paths is equal to the K-factor measured in dB. After the power of the
 25 component is added, the total power in the channel is normalized to unity power. The K-factor
 26 is defined as the ratio of power in the LOS component to the total power in the diffused
 27 component. The LOS path will coincide in time with the first (earliest) diffused path.
 28 pairing sub-rays between transmitter and receiver, the direct components are
 29 representing the LOS path.

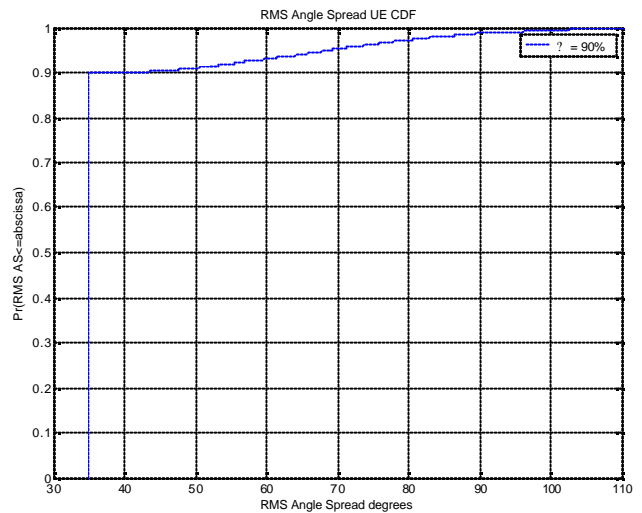
30 3.5.4 Urban canyon

31 The urban canyon model is switch selectable. When switched on, the model modifies the
 32 generation of the paths arriving at the subscriber unit. It is for use in both the urban macro and
 33 micro scenarios.

34 Urban-canyons exist in dense urban areas served by macro-cells, and for at-rooftop
 35 cells. When this model is used, the spatial channel for all subscribers in the simulation
 36 universe will be defined by the statistical model given below. Thus for the SCM channel
 37 generation steps given in Section 3.3, Step 9 is replaced with steps 9a-d given below,
 38 describe the AoAs of the paths arriving at the subscriber in the urban canyon scenario.

- 1 The following procedure is used to determine the subscriber mean AoAs of the six paths.
- 2 model does not use a building grid, but assigns angles based on statistical data present
- 3 the figures below. The procedure is defined in terms of the subscriber terminal:
- 4 9a. Select a random street orientation from: $U(0, 360^\circ)$ which also equals the direction of
- 5 for the UE.
- 6 9b. Select a random orientation for the subscriber antenna array from $U(0, 360)$.
- 7 9c. Given η the predefined fraction of UEs to experience the urban canyon effect. Set
- 8 uniform random draw for the parameter η .
- 9 9d. If $\eta \leq \eta_{draw}$ select the UE AoAs for all arriving paths to be equal, with 50% probability of
- 10 from the direction of the street orientation obtained in step 9a, and 50% the
- 11 orientation plus an offset of 180° . If $\eta > \eta_{draw}$ select the directions of arrival for all paths
- 12 the standard SCM UE AoA model given in Section 3.3, Step 9.

13



14

15

Figure 3-3. Simulated results of urban canyon algorithm

16 In **Figure 3-3**, the urban canyon procedure is simulated to show the effects of the model on
 17 composite UE angle spread. The parameter η , which describes the percentage of UEs that
 18 will experience the urban canyon effects. The figure illustrates the result of selecting
 19 AoAs, where each of the paths has a fixed 35° angle spread.

20 The parameter η , is set to a relatively high percentage of occurrence to emphasize
 21 urban canyon effects, while the remaining occurrences assume some mixed arrivals to
 22 various other conditions such as cross streets or where signals arrive from between buildings
 23 or from unknown paths at various angles.

1 **3.6 Correlation Between Channel Parameters**

2 In [1], Greenstein presents a model for correlating delay spread (DS) with log normal shadow fading (LN). Since both are shown to be log-normal distributed, the correlation between DS and LN are correlated by the coefficient $\rho_{DS, LN}$. The best value for suburban and urban data shown to be $\rho_{DS, LN} = -0.75$, presented in [1] from data measured by [2].

6 The result of the correlation between log normal shadowing and delay spread is significant because it indicates that for a strong signal (positive LN), the DS is reduced, and for a weak signal condition (negative LN), the DS is increased.

9 Cost 259[3] presents the azimuth spread (AS) as also being log-normal distributed and likewise being correlated to the DS and LN. Since the correlation of these parameters is high, a spatial channel model needs to be specified that can reproduce this correlated behavior along with the expected probability and range of each parameter. For a macro environment, the following values are given in [3]:

14

15 $\rho_{DS, AS} = \text{Correlation between DS \& AS} = +0.5$

16 $\rho_{LN, AS} = \text{Correlation between LN \& AS} = -0.75$

17 $\rho_{LN, DS} = \text{Correlation between LN \& DS} = -0.75$

18

19 Suppose we wish to generate the values for DS, AS, and LN for the n th base station ($n = 1, 2, \dots, N$) with respect to a given mobile user. These values are given as $\rho_{DS,n}, \rho_{AS,n}$, and $\rho_{LN,n}$ respectively. These values are a function of the respective correlated Gaussian random variables $\rho_{DS,n}, \rho_{AS,n}$, and $\rho_{LN,n}$. These correlated Gaussian random variables are in turn respectively generated from independent Gaussian random variables w_{n1}, w_{n2} , and w_{n3} . Note however that because of correlated shadow fading from base to base, the variables w_{n3} through w_{N3} are correlated and are given by:

26

$$w_{n3} = \rho_{c,3} \sqrt{\frac{\rho_{c,3}}{c_{33}}} \rho_{n3} \sqrt{1 - \frac{\rho_{c,3}^2}{c_{33}}}, \quad n = 1 \dots N$$

27 where $\rho_{c,1}, \rho_{c,2}, \dots, \rho_{c,N}$ are i.i.d. Gaussian random variables with zero mean and unit variance. $\rho_{c,3}$ is the site-to-site correlation (assumed to be $\rho_{c,3} = 0.5$), and c_{33} is defined as the lower triangular component of the matrix square root of the correlation matrix:

30

$$\begin{bmatrix} \rho_{c,1} & c_{12} & c_{13} & \rho_{c,1} \rho_{c,2} & \rho_{c,1} \rho_{c,3} & \rho_{c,1} \rho_{c,2} \rho_{c,3}^{1/2} \\ \rho_{c,2} & c_{22} & c_{23} & \rho_{c,2} \rho_{c,3} & \rho_{c,2} \rho_{c,3} & \rho_{c,2} \rho_{c,3} \\ \rho_{c,3} & c_{32} & c_{33} & \rho_{c,3} & \rho_{c,3} & \rho_{c,3} \end{bmatrix}$$

31 Given w_{n3} , generate i.i.d. Gaussian random variables w_{n1} and w_{n2} with zero mean and unit variance. The variables $\rho_{DS,n}, \rho_{AS,n}$, and $\rho_{LN,n}$ are given by:

33

$$\begin{bmatrix} \rho_{DS,n} \\ \rho_{AS,n} \\ \rho_{LN,n} \end{bmatrix} = \begin{bmatrix} \rho_{c,1} & c_{12} & c_{13} \\ \rho_{c,2} & c_{22} & c_{23} \\ \rho_{c,3} & c_{32} & c_{33} \end{bmatrix} \begin{bmatrix} w_{n1} \\ w_{n2} \\ w_{n3} \end{bmatrix}$$

1 The distribution of DS for the n th BS is given by:

$$2 \quad P_{DS,n} = 10^{\mu_{DS,n} + \sigma_{DS,n} \epsilon_n} \quad (3.10)$$

3 where ϵ_n is generated above, $\mu_{DS} = E\{\log_{10}(P_{DS})\}$ is the logarithmic mean of the distribut
4 DS, and $\sigma_{DS} = \sqrt{E\{\log_{10}(P_{DS}^2)\} - \mu_{DS}^2}$ is the logarithmic standard deviation of the distri
5 of DS.

6 Similarly the distribution of AS is given by:

$$7 \quad P_{AS,n} = 10^{\mu_{AS,n} + \sigma_{AS,n} \epsilon_n} \quad (3.11)$$

8 where ϵ_n is generated above, $\mu_{AS} = E\{\log_{10}(P_{AS})\}$ is the logarithmic mean of the distribut
9 AS, and $\sigma_{AS} = \sqrt{E\{\log_{10}(P_{AS}^2)\} - \mu_{AS}^2}$ is the logarithmic standard deviation of the distribut
10 AS.

11 Finally, the distribution for the LN is given by:

$$12 \quad P_{LN,n} = 10^{\mu_{LN,n} + \sigma_{LN,n} \epsilon_n} \quad (3.12)$$

13 where ϵ_n is given above, and σ_{LN} is the LN standard deviation given in dB. The value of
14 obtained from analysis of the standard deviation from the regression line of the path
15 versus distance. As shown in Table 3-1, these values are 8dB and 10dB for the macr
16 microcell cases, respectively. Note that the linear scale value for LN is simply $10^{\sigma_{LN}/10}$.

17 3.7 Modeling intercell interference

18 Sophisticated MIMO receivers, such as those based on minimum mean-squared error s
19 processing, account for the spatial characteristics of the signals from the desired sector a
20 as from the interfering sectors. The spatial characteristics of these signals can be mo
21 according to the channel matrix generated according to Sections 3.3, 3.4, and 3.5. Howe
22 may be prohibitively complex to explicitly model the spatial characteristics of all inter
23 sectors, especially those whose received powers are relatively weak. It has been shown th
24 modeling the signals of relatively weak interferers as spatially white (and thereby ignorin
25 spatial characteristics), the resulting performance difference is negligible. The followin
26 steps outline the procedure for modeling intercell interference.

27

28 ?? Determine the pathloss and shadowing of all sectors. (Note that "pathloss" imp
29 includes antenna patterns as well.)

30 ?? Rank the sectors in order of received power (based on pathloss and shadowing).

31 ?? Assign the strongest sector as the serving sector.

32 ?? Model the next strongest B sectors as spatially correlated Gaussian noise processes
33 covariances are determined by their channel matrices. These channel matrices
34 generated from Sections 3.3, 3.4, and 3.5 and account for the pathloss, shadowing
35 fast fading variations.

1 ?? Model the remaining sectors as spatially white Gaussian noise processes whose vari
 2 are based on a flat Rayleigh fading process. Hence the variances are varying ove
 3 duration of a simulation drop.

4

5 Using the notation in Appendix A, suppose there are J transmit antennas, M receive ante
 6 N is the receiver tap length, and K is the impulse response length. In modeling the B str
 7 interfering sectors, let \mathbf{G} be the MN by $(N+K-1)J$ MIMO channel impulse response matrix
 8 by

9

$$\mathbf{G} = \begin{bmatrix} \mathbf{G}_1^{(1)} & \dots & \mathbf{G}_1^{(J)} \\ \vdots & \ddots & \vdots \\ \mathbf{G}_M^{(1)} & \dots & \mathbf{G}_M^{(J)} \end{bmatrix}$$

11

12 Hence, assuming the data symbols are normalized to have unit power, the equivalent Gau
 13 vector noise process is an MN -dimensional complex Gaussian random variable with zero
 14 and covariance $\mathbf{G}\mathbf{G}^H$, where superscript H denotes the Hermitian transpose.

15 To model the remaining "weak" sectors, we assume that the mean power of the flat Ra
 16 fading process is equal to the effects of pathloss and shadowing from each sector. There
 17 the received power from the b th sector due to pathloss and shadowing is P_b , then the Ra
 18 fading process for the m th receive antenna ($m = 1, \dots, M$) as a function of time is given by
 19 where the mean of $r_{b,m}(t)$ over time is P_b . The fading processes for each sector and r
 20 antenna are independent, and the doppler rate is determined by the speed of the mobil
 21 assume that the fading is equivalent for each mobile receive antenna. The total received
 22 power per receive antenna due to all "weak" sectors at the m th antenna is

$$\sum_{b \in F} r_{b,m}(t)$$

24 where F is the set of indices for the "weak" sectors.

25 For 3-sector systems, we model the $B = 8$ strongest sectors. For 6-sector systems, we moc
 26 12 strongest sectors. The values for B are based on simulation results for the typical cell l
 27 with a single hexagonal cell surrounded by two rings of cells (a total of 19 cells) and with
 28 placed in the center cell. For other layouts, different values of B or an entirely diff
 29 technique may be required to properly account for the intercell interference.

30 **3.8 System Level Calibration**

31 The following examples are given for calibration purposes. A resolvable path at the recei
 32 assumed to be the energy from one (or more) paths falling within one chip interval. The
 33 rate in UMTS is 3.84Mcps. The PDF of the number of resulting resolvable paths is recorde

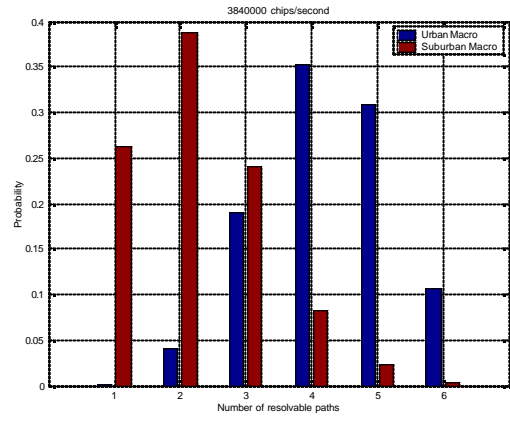
34 The following table is for interim calibration purposes. "Ideal" signifies the value take
 35 measurements, "Input" signifies the value used in generating a random variable, "O
 36 signifies the resulting measured statistic.

1

Parameter	Suburban 5? ? RND = 3dB		Urban 8? ? RND = 3dB		Urban 15? ? RND = 3dB		Urban
	Input	Output	Input	Output	Input	Output	
r_{DS}	1.4	1.29	1.7	1.54	1.7	1.54	
σ_{DS}	Input	Ideal	Input	Ideal	Input	Ideal	
	-6.80	-6.92	-6.18	-6.26	-6.195	-6.26	
σ_{DS}	Input	Ideal	Input	Ideal	Input	Ideal	
	0.288	0.363	0.18	0.25	0.18	0.25	
r_{AS}	Input	Output	Input	Output	Input	Output	
	1.2	1.22	1.3	1.37	1.3	1.37	
σ_{AS}	Input	Ideal	Input	Ideal	Input	Ideal	
	0.69	0.66	0.810	0.75	1.18	1.0938	
σ_{AS}	Input	Ideal	Input	Ideal	Input	Ideal	
	0.13	0.18	0.34	0.37	0.21	0.2669	
$E[\sigma_{DS}]$	Ideal	Output	Ideal	Output	Ideal	Output	
	0.17?s	0.172?s	0.65?s	0.63?s	0.65?s	0.63?s	
$E[\sigma_{AS} \text{ Node B}]$	Ideal	Output	Ideal	Output	Ideal	Output	Ideal
	5?	5.01?	8?	7.97?	15?	14.9?	19°
$E[\sigma_{AS} \text{ UE}]$	Ideal	Output	Ideal	Output	Ideal	Output	Ideal
	72?	72.59?	72?	71.49?	72?	71.35?	72?

2 Table 3-3. SCM parameter summary with simulated outputs

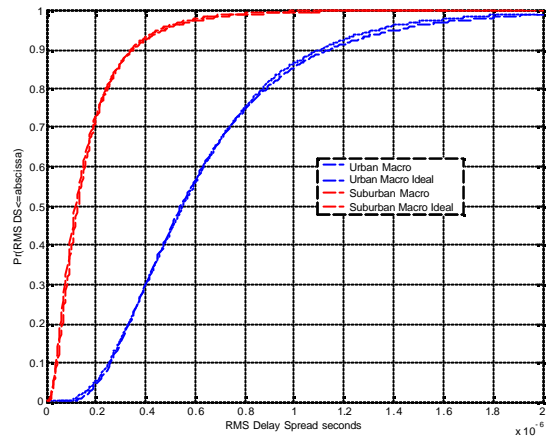
3 The following figures: Figure 3-4, Figure 3-5, Figure 3-6, Figure 3-7, Figure 3-8, represent
 4 calibration cases for the current SCM model. These curves correspond to the parameters
 5 presented in Table 3-3, and include the 3dB randomizing factor for the generation of
 6 powers.



1

2

Figure 3-4. Probability of urban and suburban time resolvable paths



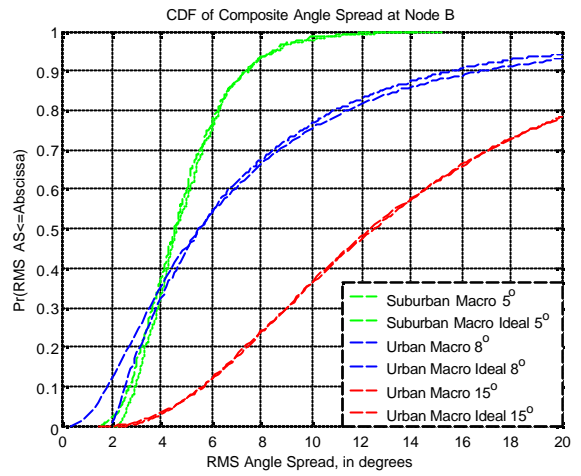
3

4

5

6

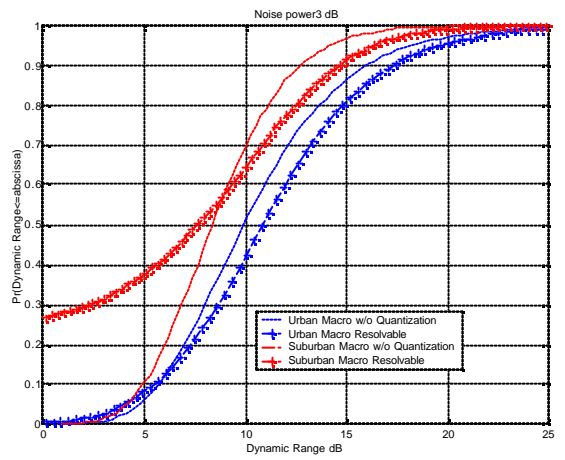
Figure 3-5. RMS delay spread, simulated versus ideal



1

2

Figure 3-6. BS composite angle spread, simulated versus ideal

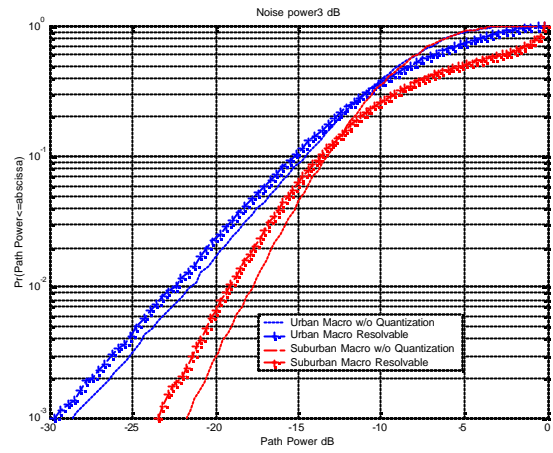


3

4

5

Figure 3-7. Dynamic range (dB) for each channel model



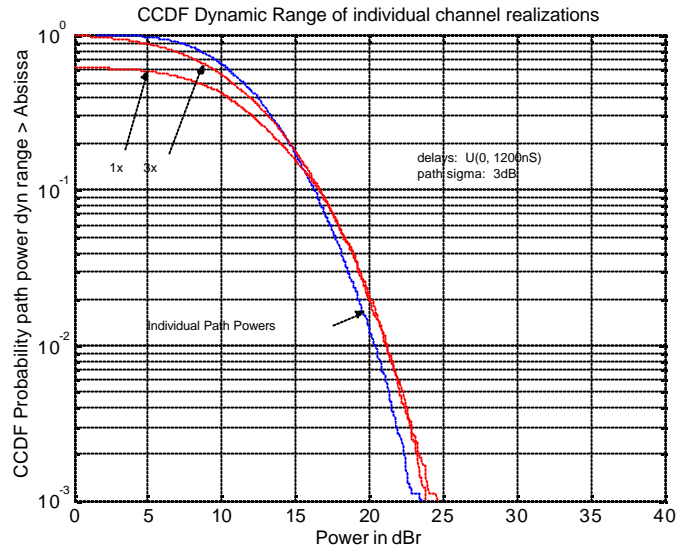
1
2
3

Figure 3-8. CDF of all path powers

1 Channel Scenario: Urban Microcellular

2

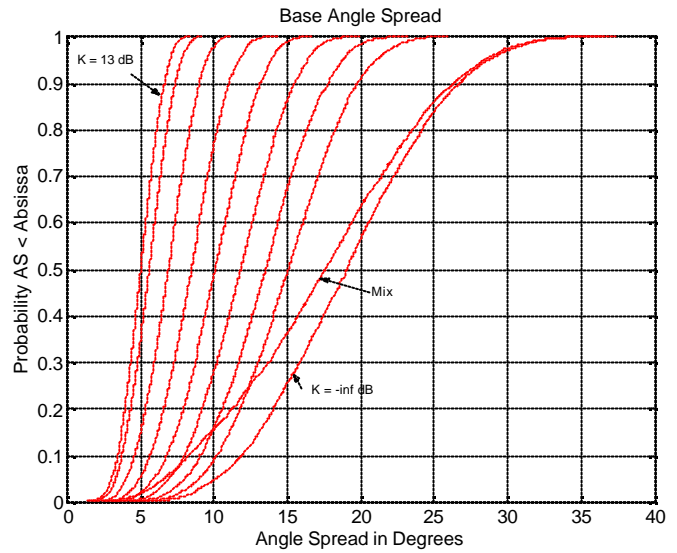
3 A number of parameters are shown in the following plots which are the result of simula
 4 Figure 3-9 illustrates the dynamic range of each channel realization, plotted
 5 complementary cdf. The difference between the 1x and 3x channel bandwidths are shc
 6 the resolvable dynamic range curves. (Powers are combined within a chip time as a simpl
 7 to estimate the resolvable powers.) The 1% highest value is approximately the same for
 8 bandwidths. The dynamic range D is calculated from $D = 10 \cdot \log_{10}(\max \text{ pwr} / \min \text{ pwr})$
 9 each channel realization.



10

11

Figure 3-9. Dynamic range of path powers per channel realization, (NLOS)



1

2

Figure 3-10. Composite BS angle spread

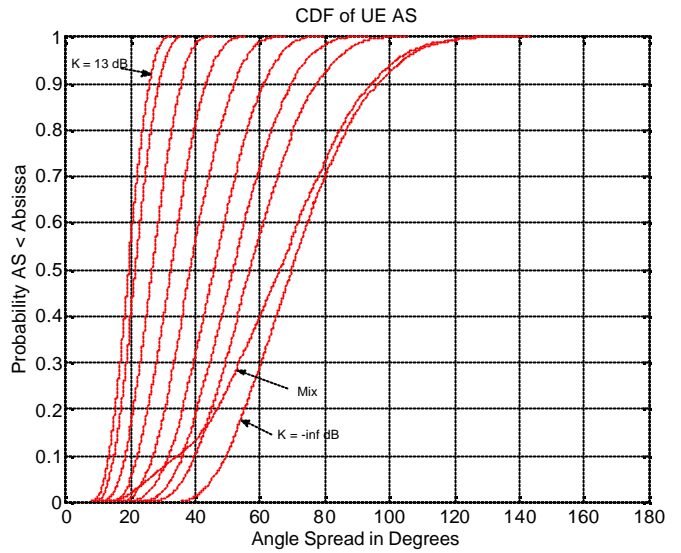
3

The composite angle spread at the base is described in Figure 3-10 for the various K-factors that are seen in the micro-cell model, along with the LOS/NLOS mix expected when the radius is 500m. For the NLOS case, the average composite Base AS = 19.2°. When experienced LOS paths with increased K-factors, the angle spreads are observed to decrease accordingly. The simulated average composite Base AS for the NLOS model is: 19.2°, and the simulated average composite Base AS for the mixed propagation model is: 17.6°.

6

7

8



1

2

Figure 3-11. Composite MS angle spread

3

The composite UE angle spread is described in Figure 3-11 for the various K-factors that are present in the micro-cell model. Increased K-factor from a LOS path, causes the composite angle spread to be decreased since more power is present in a single direct component. The mixed case shown which has a slight decrease in the statistics due to the 15% of the locations experiencing the LOS condition. The simulated composite UE AS for the NLOS model is: 71.8°, and the simulated composite UE AS for the mixed propagation model is: 65.8°.

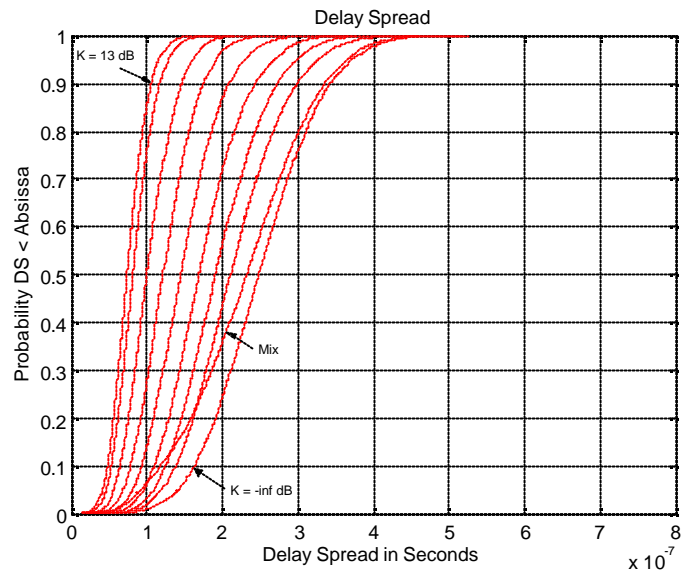
9

The delay spread is illustrated in Figure 3-12, which is also affected by the presence of a LOS path. The mixed case is produced by the combination of LOS and NLOS paths. The simulated average delay spread for the NLOS condition is: 251 nS, and the simulated average delay spread for the mixed case is: 231 nS

10

11

12



1

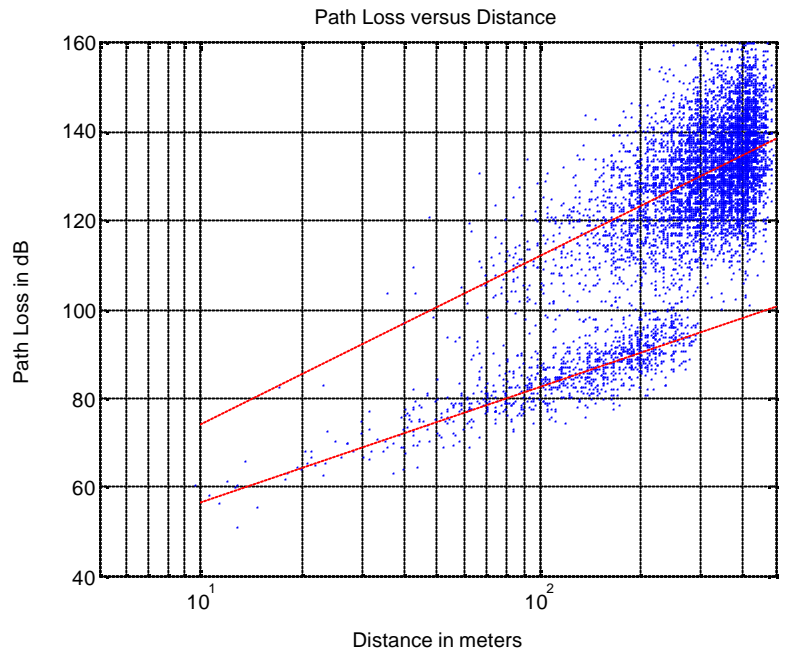
2

Figure 3-12. Micro-cell delay spread

3

Figure 3-13 illustrates the propagation path loss model of the Urban Micro-cell which is characterized by the mixed mode between LOS and NLOS.

4



1

Figure 3-13, Microcell path loss versus distance

2

3 **ANNEX A: MMSE RECEIVER DESCRIPTION**

4 The following text is a preliminary description of the MMSE receiver. The receiver d
 5 described here are example receiver structures. They do not imply their use for min
 6 performance requirements. Their use in calibration or system level simulations i
 7 mandatory.

8 This procedure generates SINR values at the output of a linear MMSE receiver for a :
 9 instant in time.

10 *Step 1: Given the space-time propagation model and transmitter state, form a channel (exp*
 11 *here as one or more convolution matrices) relating all transmitting sources and re*
 12 *antennas from every sector in the system.*

13 At the UE, the received samples are represented as a column vector,

14

$$\mathbf{r} = [\mathbf{r}_1^T, \mathbf{r}_2^T, \dots, \mathbf{r}_M^T]^T$$

$$= [r_1(1), r_1(2), \dots, r_1(N), r_2(1), r_2(2), \dots, r_2(N), \dots, r_M(1), r_M(2), \dots, r_M(N)]^T,$$

1 where M is the number of receive antennas at the UE, and N is the number of rec
 2 symbols per antenna¹. This received time-space vector is related to the trans
 3 symbols as follows:

$$4 \quad \mathbf{r} = \mathbf{G}^{(1)} \mathbf{x}^{(1)} + \sum_{j=2}^J \mathbf{G}^{(j)} \mathbf{x}^{(j)} + \mathbf{n}$$

$$\begin{matrix} \mathbf{G}_1^{(1)} & & \mathbf{G}_1^{(j)} & & \mathbf{n}_1 \\ \mathbf{G}_2^{(1)} & & \mathbf{G}_2^{(j)} & & \mathbf{n}_2 \\ \vdots & & \vdots & & \vdots \\ \mathbf{G}_M^{(1)} & & \mathbf{G}_M^{(j)} & & \mathbf{n}_M \end{matrix}$$

5 where $\mathbf{G}_i^{(j)}$, $1 = i, j = M$ are Toeplitz convolution matrices defining the channel between
 6 th receive antenna and the j -th transmitted data stream, $\mathbf{x}^{(j)}$ is the j -th transmitte
 7 stream, J is the total number of data streams in the system, and \mathbf{n} is the vector of rec
 8 samples. The $j = 1$ data stream is the primary data stream intended for the user. Th
 9 data stream can be a transmission from an interfering base station, another sector
 10 desired base station, or another data stream intended for the desired user (whi
 11 considered interference to the primary data stream). If the composite channel respo
 12 limited to K samples, then each of the convolution matrices has N rows by $(N+K-1)$ col

$$13 \quad \mathbf{G}_i^{(j)} = \begin{bmatrix} g_i^{(j)}(K) & g_i^{(j)}(K-1) & \dots & g_i^{(j)}(1) & 0 & \dots & 0 & \dots \\ 0 & g_i^{(j)}(K) & g_i^{(j)}(K-1) & \dots & g_i^{(j)}(1) & 0 & \dots & 0 \\ \vdots & \vdots & \vdots & \vdots & \vdots & \vdots & \vdots & \vdots \\ 0 & 0 & \dots & 0 & g_i^{(j)}(K) & g_i^{(j)}(K-1) & \dots & g_i^{(j)}(1) \end{bmatrix},$$

14 and $\mathbf{g}_i^{(j)}$ is the vector of discrete channel samples of length K .

15 Note that in the above formulation, the vector \mathbf{x} has $M(N+K-1)$ rows, and thus, it is l
 16 than the received vector, \mathbf{r} . Also, the vector \mathbf{x} will be interleaved with zero value
 17 fractionally-spaced approach with more than one received sample per symbol is used.

18 *Step 2: Using the above channel, produce an estimate of the channel.*

$$19 \quad \hat{\mathbf{g}}_i^{(j)} = \mathbf{g}_i^{(j)} + \mathbf{g}_i^{(j)},$$

20 where $\mathbf{g}_i^{(j)}$ is a vector representing the channel estimation error for the i -th r
 21 antenna and the j -th transmitted data stream. The estimation error is due to nois
 22 interference in the pilot channel and can also be due to the channel estimator's inabi
 23 track a fast fading channel.

24 *Step 3: Using the estimated channel, compute the SINR per data stream at the output*
 25 *MMSE filters.*

$$26 \quad SINR_j = \frac{\mathbf{f}_j^H \hat{\mathbf{O}}_j^{-1} \hat{\mathbf{f}}_j}{\hat{\mathbf{f}}_j^H \hat{\mathbf{O}}_j^{-1} \mathbf{O}_j \hat{\mathbf{O}}_j^{-1} \hat{\mathbf{f}}_j},$$

27 where

¹ Actually, this is the number of received samples per antenna, if more than one sample per syn
 collected.

$$\mathbf{O}_j = \mathbf{G}^{(j)} E \mathbf{x}^{(j)} \mathbf{x}^{(j)H} \mathbf{G}^{(j)H} + \mathbf{f}^{(j)} E \mathbf{x}^{(j)} (d) \mathbf{x}^{(j)} (d) \mathbf{f}^{(j)H} + \sum_{m=1}^J \mathbf{G}^{(m)} E \mathbf{x}^{(m)} \mathbf{x}^{(m)H} \mathbf{G}^{(m)H} + E \mathbf{n} \mathbf{n}^H$$

$\hat{\mathbf{O}}_j$ is an estimate of \mathbf{O}_j , $d = \max\{N - K, K\}$, \mathbf{f}_j is the d -th column of $\mathbf{G}^{(j)}$, $x^{(j)}$ the d -th element (desired symbol) of the $\mathbf{x}^{(j)}$ data stream vector, and $SINR_j$ represents the for the j -th transmitted data stream in the system. In this example, the primary data sent to a user will be $j = 1$. In a MIMO system where multiple data streams are sent to a user, the second stream could be $j = 2$, etc.

7

ANNEX B: CHANGE HISTORY

Change history						
Date	TSG #	TSG Doc.	CR	Rev	Subject/Comment	Old

9